

Cherenkov light imaging in astroparticle physics

U. F. Katz

Erlangen Centre for Astroparticle Physics, Friedrich-Alexander University Erlangen-Nürnberg, Erwin-Rommel-Str. 1, 91058 Erlangen, Germany

Abstract

Cherenkov light induced by fast charged particles in transparent dielectric media such as air or water is exploited by a variety of experimental techniques to detect and measure extraterrestrial particles impinging on Earth. A selection of detection principles is discussed and corresponding experiments are presented together with breakthrough-results they achieved. Some future developments are highlighted.

Keywords: Astroparticle physics, Cherenkov detectors, neutrino telescopes, gamma-ray telescopes, cosmic-ray detectors

1. Introduction

In 2018, we commemorate the 60th anniversary of the award of the Nobel Prize to Pavel Alexeyewich Cherenkov, Ilya Mikhailovich Frank and Igor Yevgenyevich Tamm for *the discovery and the interpretation of the Cherenkov effect* [1, 2]. The impact of this discovery on astroparticle physics is enormous and persistent. Cherenkov detection techniques were instrumental for the discovery of neutrino oscillations; the detection of high-energy cosmic neutrinos; the establishment of ground-based gamma-ray astronomy; and important for the progress in cosmic-ray physics.

The characteristics of Cherenkov radiation are governed by its emission angle with respect to the particle's direction of flight, $\cos \theta_C = 1/(n\beta)$ (n and $\beta = v/c$ being the refractive index and the particle velocity, respectively) and by its intensity, given by the Frank-Tamm formula

$$\frac{dN_\gamma}{dx} = 2\pi\alpha \left(1 - \frac{1}{\beta^2 n^2}\right) \cdot \left(\frac{1}{\lambda_{\min}} - \frac{1}{\lambda_{\max}}\right)$$
$$\beta \approx \begin{cases} 3 \times 10^4 / \text{m} & \text{in water/ice} \\ 15 / \text{m} & \text{in air (8 km height)} \end{cases}$$
$$\text{for } \lambda_{\min} = 300 \text{ nm} \leq \lambda \leq \lambda_{\max} = 600 \text{ nm}.$$

Here, λ is the emitted wavelength and the λ range indicated roughly corresponds to the sensitivity range of typical light sensors. The geometry of Cherenkov emission allows for reconstructing the particle trajectory, provided sufficiently many Cherenkov photons are measured with good spatial and time resolution, and they can be separated from background light. The recorded Cherenkov intensity furthermore can serve as a proxy for the particle energy. Usually, the detectors need to be shielded from ambient light and employ photo-sensors that are sensitive to single photons with nanosecond time resolution.

Photomultiplier tubes (PMTs) and, more recently, silicon photomultipliers (SiPMs) [3, 4] are the standard sensor types. They are provided by specialised companies who cooperate with the experiments in developing and optimising sensors according to the respective specific needs (see e.g. [5, 6]).

In the following, the detection principles of different types of Cherenkov experiments in astroparticle physics are presented together with selected technical details and outstanding results.

2. Ground-based gamma-ray detectors

While the atmosphere is transparent to electromagnetic radiation in the radio and optical regimes, it is not for X-rays and gamma-rays. Gamma-rays below 20 GeV are only accessible to satellite experiments. At significantly higher energies, satellite instruments rapidly lose sensitivity to the steeply decreasing gamma-ray flux due to their limited collection area, and ground-based observations take over (see [7] for more details). Imaging air Cherenkov telescopes (IACTs) require clear, preferentially moon-less nights and sites with negligible light pollution and an elevation of typically 2 km. They are pointing instruments with a field of view of a few degrees in diameter. Alternatively, timing arrays at higher altitude can directly measure the gamma-induced particle cascade. They cover a significant fraction of the sky, albeit with a higher energy threshold than IACTs and inferior sensitivity at energies below about 50 TeV.

2.1. Detection principle of Cherenkov telescopes

Upon entering the atmosphere, gamma-rays with GeV energies and above initiate electromagnetic cascades, extending longitudinally over several kilometres and having their maximum typically at a height of 10 km above sea level. The integrated track length of all e^\pm in the cascade and therefore the overall Cherenkov light yield is to a good approximation proportional to the initial gamma-ray energy, E_γ . The Cherenkov angle is about $\theta_C = 1^\circ$ and increases with the air density, i.e.

Email address: katz@physik.uni-erlangen.de (U. F. Katz)

along the cascade. Even though the basic processes in the cascade – pair creation and bremsstrahlung – are very close to being collinear with the incoming gamma-ray, multiple scattering of the e^\pm widens the Cherenkov light pool, which is concentrated within a radius of about 100–150 m at ground level.

Since all relevant particles in the cascade propagate with a speed very close to that of light, the Cherenkov radiation arrives at ground in a flash of only a few nanoseconds duration and can thus be separated from the night-sky background. It is observed with one or several IACTs that have a camera made of photomultiplier or SiPM pixels in their focal plane. An important parameter, governing e.g. the ability for large-area sky scans, is the field of view of the camera (a few degrees). Each camera pixel corresponds to a certain solid angle of the light arrival direction. A telescope pointed to a gamma-ray source thus sees the start of the cascade (small θ_C , little multiple scattering) close to its centre, from where it propagates outward. An example of a cascade observed by all five H.E.S.S. telescopes (see Sect. 2.2) is shown in Fig. 1. The gamma-ray direction and energy are reconstructed from the recorded light pattern and intensity. Typical resolutions of 0.1° and 20%, respectively, are achieved for stereoscopic observations by several cameras. Atmospheric cascades induced by cosmic-ray protons or heavier nuclei are three orders of magnitude more frequent than gamma-rays, but can be efficiently suppressed using the topology of the camera pictures (hadronic showers are more fuzzy).

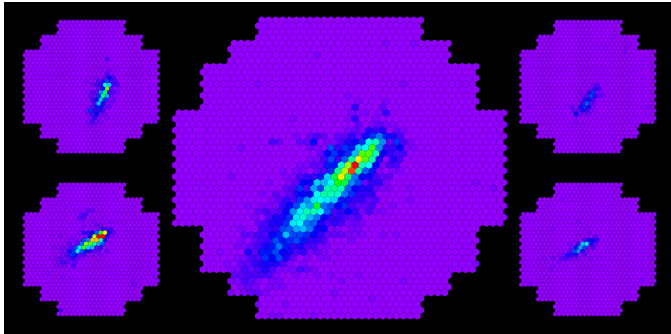


Figure 1: Camera pictures of a gamma-ray shower simultaneously observed by all five H.E.S.S. telescopes. Each hexagonal pixel corresponds to one photomultiplier. The colour code indicates the measured light intensity. Picture provided by the H.E.S.S. Collaboration.

The observable E_γ range is limited by the light intensity and the background separation at low energies (some 10 GeV for the largest telescopes in operation) and by the overall collection area at high energies (about 100 TeV for a large array of smaller telescopes). The sensitivities of current and future gamma-ray telescopes are compared in Fig. 2 as functions of E_γ .

2.2. Current Cherenkov telescopes

After the feasibility of ground-based gamma-ray astronomy had been demonstrated in the late 1980's and 1990's by the Whipple [11] and HEGRA [12] instruments, a second generation of IACTs became operational in the 2000's. The main

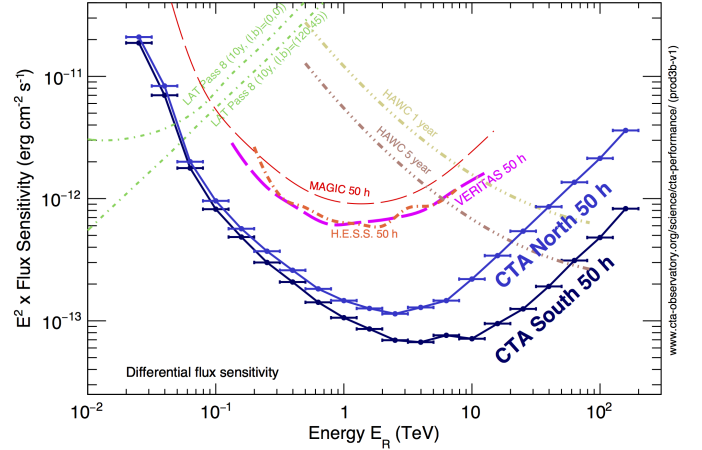


Figure 2: Differential flux sensitivity of the current (H.E.S.S., MAGIC, VERITAS) and the future (CTA) ground-based IACTs. Also shown are the corresponding sensitivities for the timing array HAWC. See Sections 2.2–2.4 for more details on these instruments. The green, dash-dotted lines indicate the sensitivity of the satellite instrument Fermi-LAT for two different directions of observation. See Sections 2.2–2.4 for more details on these instruments. Note that the vertical axis shows $E_\gamma^2 \cdot \text{flux}$. Picture provided by the CTA Collaboration.

properties of these telescopes are summarised in Table 1; a photograph of the H.E.S.S. instrument is shown in Fig. 3. They have established gamma-ray astronomy as a major field of observational astrophysics and provided a wealth of scientific information on high-energy processes in the Universe. More than 200 gamma-ray sources in the TeV regime have been detected and their spectra, light curves and – for Galactic sources – morphologies investigated. Gamma-ray emission and thus particle acceleration beyond TeV energies has been proven for a number of object classes, amongst them shell-type supernova remnants, pulsar wind nebulae, compact binaries and active galactic nuclei. See [7] and references therein for details.

In addition to the IACTs listed in Table 1, a first small telescope with a camera equipped with SiPMs, FACT [13], has been constructed and is operated since 2011 in La Palma for long-term monitoring purposes. FACT has demonstrated that SiPMs can take very high rates, enabling observations even in full-moon nights.

2.3. Cherenkov Telescope Array

The H.E.S.S., MAGIC and Veritas collaborations have joined forces to construct the next-generation IACT, the Cherenkov Telescope Array (CTA). CTA will be installed in two sites, one in the Northern hemisphere on La Palma and the other in the Southern hemisphere close to the ESO Paranal Observatory in Chile. CTA will consist of telescopes of three sizes, LSTs (large size telescopes), MSTs (medium) [14] and SSTs (small) [15], with a field of view of 4.5° (LST) and 8° (MST and SST), respectively. At the Chile site, they will be arranged in concentric groups of 4 LSTs in the middle, followed by 25 MSTs and 70 SSTs. On La Palma, there will be 4 LSTs and 15 MSTs, but



Figure 3: Photograph of the H.E.S.S. telescope system in Namibia. Picture provided by the H.E.S.S. Collaboration.

Table 1: Main parameters of the currently operational IACTs and references to their web pages. The second MAGIC telescope came in operation 2009, the large H.E.S.S. telescope in 2012.

	H.E.S.S.	MAGIC	Veritas
Site	Namibia	La Palma, Spain	Arizona, US
Altitude a.s.l.	1800 m	2200 m	1270 m
Operation	2003–	2004–	2007–
Telescopes	5	2	4
Dish diameter	4×12 m, 1×28 m	2×17 m	4×12 m
Field of view	5°	3.5°	3.5°
Photo-sensors	PMTs	PMTs	PMTs
Web page	[8]	[9]	[10]

no SSTs. This takes into account that on the Northern site predominantly extragalactic observations will be made, where the gamma-ray flux beyond some 10 TeV – targeted by the SSTs – is strongly reduced through absorption by the extragalactic background light. The first LST was recently inaugurated in La Palma. CTA is expected to start operation in 2022 with partial arrays and to be completed in 2025. The CTA sensitivity (see Fig. 2) promises major progress in gamma-ray astronomy and high-energy astrophysics once CTA will take data.

The major scientific targets of CTA are cosmic particle acceleration, probing extreme environments such as close to neutron stars and black holes, and fundamental physics such as investigations into the nature of dark matter. CTA will be operated as an observatory, with some key science projects reserved for the CTA Collaboration. These include surveys of the Galactic Centre, the Galactic Plane, the Magellanic Cloud, and extragalactic objects, as well as the investigation of cosmic-ray PeVatrons, star-forming galaxies, active galactic nuclei and clusters of galaxies. Also, the dark matter programme and the exploitation of CTA data beyond gamma-rays are key science projects.

2.4. Timing arrays

At altitudes exceeding about 4 km above sea level, the particle cascades induced by gamma-rays and cosmic rays at energies beyond 100 GeV reach the ground and can be observed with arrays of suitable detectors, e.g. water tanks in which through-going charged particles generate Cherenkov light detected by PMTs. From measuring the arrival time of the shower front as a function of the horizontal position, the direction of the incoming particle can be determined. The intensity of the shower and the size of its footprint on ground yield an energy estimate. Similarly to IACTs, leptonic and hadronic showers are separated using the different event topologies and muon content in the detector array.



Figure 4: Photograph of the HAWC detector array in Mexico. Picture provided by the HAWC Collaboration.

The currently most sensitive detector of this type is HAWC [16] near Puebla in Mexico, at an altitude of 4100 m. HAWC consists of 300 water tanks covering 0.05 km², each filled with 200 tons of ultra-pure water observed by 4 PMTs. A photograph of HAWC is shown in Fig. 4. HAWC reaches an angular resolution of about 0.1° for gamma-ray energies $E_\gamma \gtrsim 10$ TeV. Even though, for $E_\gamma \lesssim 100$ TeV, HAWC is less sensitive than CTA for any given direction, it has the advantage of a large field of view and a very high duty cycle. It is particularly well suited to observe very high-energy gamma-ray emission from extended objects. As an example, a recent measurement of the TeV

gamma-ray flux from the vicinity of two pulsars has strongly constrained the hypothesis that positrons from these/such pulsars is responsible for the unexpectedly high flux of cosmic-ray positrons at Earth [17].

3. Neutrino telescopes

Due to their notoriously small interaction cross section, neutrinos are very good, long-range astrophysical messengers; on the other hand, they are difficult to detect. The basic principle of neutrino telescopes is to observe Cherenkov light from charged secondary particles emerging from neutrino reactions and passing a detector volume filled with a transparent dielectric medium and observed by an arrangement of PMTs (due to their comparatively high noise rates, SiPMs are not [yet] suited for neutrino telescopes). For the low-energy regime (typically MeV–multi-GeV), detectors are installed in deep-underground caverns and the PMTs cover a large percentage of the detector volume outer surface. For high energies (some GeV–10 PeV), naturally abundant volumes of water or ice are instrumented with three-dimensional arrays of PMTs [18].

3.1. Low-energy neutrino detectors

The neutrino fluxes observed with these detectors are those from the Sun (4–20 MeV), from supernovae (10–30 MeV), atmospheric neutrinos generated in cosmic-ray induced particle cascades (sub-GeV–TeV), and also beam neutrinos from accelerators for long-baseline experiments (GeV). The energy ranges indicate the typical observation windows of Cherenkov detectors. Note that the dominant neutrino interactions observed in these cases are different: Solar ν_e are detected via elastic $\nu_e e^- \rightarrow \nu_e e^-$ scattering, where the final-state e^- preserves the ν_e direction; supernova neutrinos are mostly visible via $\bar{\nu}_e p \rightarrow e^+ n$, with poor directional information; atmospheric (anti)neutrinos produce high-energy e^\pm or μ^\pm , the direction and particle type of which are measured in the detector. The physics questions addressed through these measurements are neutrino oscillations, the processes in the Sun and in supernovae, and searches for relic neutrinos from unresolved supernovae and for possible sterile neutrinos.

Two detectors have provided outstanding results: Super-Kamiokande (SK) in Japan [19] and the Sudbury Neutrino Observatory (SNO) [20] in Canada.

SK is installed in a cavern of a mine, with an overburden of 1000 m of rock. The detector volume is a stainless-steel vessel, about 40 m in diameter and 40 m in height, filled with 50 ktons of water. The outermost 18 ktons are used as veto layer against incoming charged particles. The inner volume is observed by more than 11000 20-inch PMTs, the veto layer by about 1900 8-inch PMTs. SK is operational since 1996, with a period of reduced sensitivity in 2001–2006 as the consequence of an accident destroying more than 50% of the large PMTs. SK has played a crucial role in the discovery and precision investigation of neutrino oscillations. While one piece of evidence came from confirming the solar neutrino deficit (i.e. the fact that less

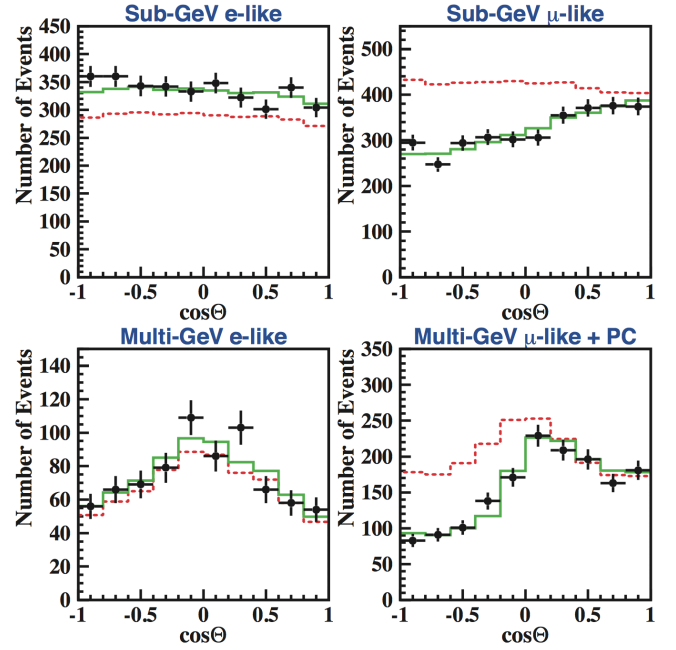


Figure 5: Zenith angle distributions for atmospheric neutrino events fully contained in the SK detector, for electron- (left) and muon-like (right) events. The upper (lower) plots are for visible energy below (above) 1.33 GeV. The high-energy muons are combined with partially contained events (PC). The error bars are the measured data, the red dotted (green solid) lines show the prediction without oscillations and with the best-fit oscillation scenario, respectively. Plot taken from [22].

solar neutrinos were measured than expected by the solar standard model), the breakthrough was the observation of oscillations of atmospheric neutrinos (see Fig. 5) in 1998. The final confirmation that the solar neutrino deficit is a neutrino flavour transition effect had to await the SNO results (see below). See [21] for a summary of recent SK results.

SNO is located below an overburden of 2100 m of rock in a deep mine in Ontario, Canada. It uses a cavity with a diameter of 22 m and a height of 34 m. The core of the detector is an acrylic vessel filled with 1 kton of heavy water (D_2O) and observed by more than 9000 8-inch PMTs. The remaining volume of the cavern is filled with normal water (H_2O), serving as a veto volume against incoming charged particles. The experiment started data taking in 1999 and was operated until 2006. Currently a follow-up experimental phase (SNO+) is in preparation, employing a liquid-scintillator filling doped with Tellurium for the search for neutrino-less double beta decay.

The deuteron target provides detectable reactions of all neutrino flavours: $\nu_e d \rightarrow e^- pp$ (charged-current), $\nu_x d \rightarrow \nu_x pn$ (neutral-current) and $\nu_x e^- \rightarrow \nu_x e^-$ (elastic, also measurable by SK). The secondary electrons are observed via their Cherenkov light, the neutrons by gamma radiation emitted when they are captured by deuterons or, in a later phase, by chlorine nuclei added through a NaCl doping. The gamma radiation Compton-scatters on electrons which then generate Cherenkov light. The measured rates of the three reactions given above allow for a

precise determination of both, the ν_e and the $\nu_\mu + \nu_\tau$ fluxes from the Sun. The overall neutrino flux is found to be consistent with the model expectation, but to consist only to about a third of electron neutrinos (see Fig. 6). This finding solved the puzzle of the solar neutrino deficit and established a consistent standard description of neutrino oscillations.

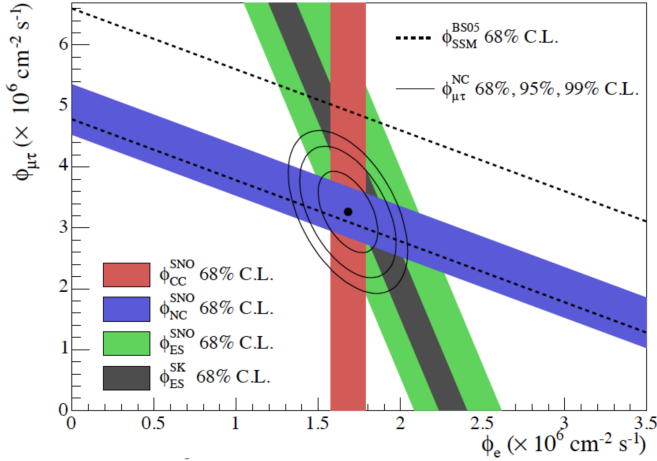


Figure 6: Solar ν_e vs. $\nu_\mu + \nu_\tau$ fluxes, with the experimental constraints by SNO indicated by the coloured bands. The grey band shows the SK result. Point and error contours are the combined result from the CC and NC measurements. The dashed lines represent the prediction by the standard solar model. Plot taken from [23].

In 2015, the Nobel Prize in physics was awarded to Takaaki Kajita (SK) and Arthur B. McDonald (SNO) for *the discovery of neutrino oscillations, which shows that neutrinos have mass*. Note that the Nobel Committee selected the pictures reproduced in Figs. 5 and 6 for the corresponding announcement.

3.2. Deep-ice and deep-water neutrino telescopes

For neutrino energies beyond some 100 GeV, the detectors discussed in the previous subsection lack sensitivity, simply because the target volume is too small to yield sufficient event rates and also because events at such energies are too large to be contained in the detector volume. In order to access this high-energy regime, in particular for the purpose of neutrino astronomy, instrumented volumes of at least several 10 Mtons, better Gtons (i.e. cubic kilometres of water/ice) are required. They are constructed by deploying arrays of vertical structures (“strings”) carrying PMTs to the deep ice of the South Pole or the deep water of the Mediterranean Sea or the Lake Baikal. The water/ice layer above the sensors completely shields the daylight. The PMTs are included in pressure-resistant glass spheres which also house the voltage supplies, the front-end electronics and calibration instruments (optical modules). The strings are connected to surface/shore by cables for data transport, operation control and electrical power supply. Particle-induced events from neutrinos or atmospheric muons are recognised and reconstructed using the space-time pattern of Cherenkov photons recorded by the optical modules. See [18] for more details.

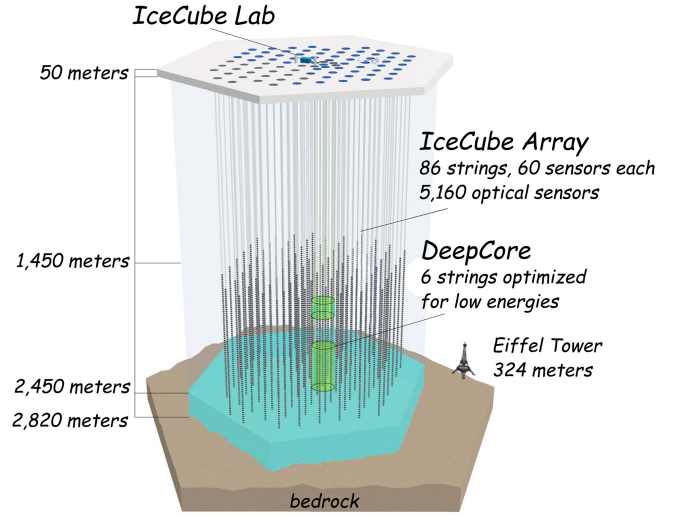


Figure 7: Schematic of the IceCube detector. Picture provided by the IceCube Collaboration.

The main science objectives of these neutrino telescopes include neutrino astronomy (i.e. observing the sky “in the light of neutrinos”); multi-messenger astronomy (i.e. combining the neutrino results with electromagnetic and gravitational wave observations); the indirect search for dark matter; neutrino and other particle physics (neutrino oscillations, neutrino interactions, etc.), the search for phenomena beyond the standard model of particle physics (magnetic monopoles, violation of Lorentz invariance, sterile neutrinos, etc.). Note that the Universe is transparent to neutrinos of all energies, whereas the reach of electromagnetic radiation is severely constrained for energies exceeding some 10 TeV due to gamma-ray interaction with ubiquitous radiation fields.

The currently most sensitive high-energy neutrino telescope is IceCube [24] at the South Pole, operational in full configuration since 2010. It consists of 86 strings carrying altogether 5160 downward-looking 10-inch PMTs instrumenting one cubic kilometre of ice at a depth between 1450 m and 2450 m. A sub-volume is instrumented more densely than the rest to detect neutrinos with energies down to 10 GeV (Deep Core, fiducial volume about 4 Mtons). The IceTop Cherenkov surface array (frozen water tanks with optical modules) serves for cosmic-ray studies and also provides some veto capability against muons and neutrinos from air showers. An in-ice hardware trigger requires hits in adjacent PMTs within 1 μs . A schematic of IceCube is shown in Fig. 7. The angular resolution for ν_μ charged-current events above some TeV is a few tenths of a degree; cascade events resulting from reactions of other neutrino flavours or neutral-current interactions are reconstructed with a resolution of about 10–15°. Main systematics come from the inhomogeneity of the optical ice properties and from light scattering, which blurs the space-time pattern of Cherenkov photons.

IceCube has achieved two major breakthrough results: The first identification and flux measurement of high-energy cosmic

neutrinos (2013) and the first association of high-energy neutrinos to an astrophysical object, the blazar TXS 0506.056 (2018). This detection became possible by relating an IceCube neutrino alert with electromagnetic observations, and was confirmed by archival IceCube data. See [25, 26] for these and further IceCube results.

The IceCube detector will be further developed and extended. As a first step, 7 additional strings with newly developed optical modules and calibration devices will be added to the Deep Core region. This project has currently been approved by the US National Science Foundation (NSF), and deployment is expected in 2022/23. The main objectives are a better understanding of the ice properties, entailing a reduction of the systematic uncertainties; improved investigation of neutrinos in the few-GeV range; test of new hardware developments. As a next step, IceCube-Gen2 with a 10 km³ deep-ice detector, a high-density core for low-energy neutrinos (PINGU), a large cosmic-ray and veto surface array, and a radio detection array is planned. If all works well, IceCube-Gen2 could be installed 2025–2031. See [25] for details.

Complementing IceCube in the field of view and in the major systematic uncertainties, the ANTARES neutrino telescope in the Mediterranean Sea off the French shore near Toulon is operational in full configuration since 2008. It consists of 12 strings carrying 25 storeys with three 10-inch PMTs each, downward-looking at an angle of 45° to vertical. The strings are connected to a junction box on the sea bed and from there by an electro-optical cable to shore. All PMT hits exceeding a signal height corresponding to 0.3 photo-electrons are read out and sent to shore, where the data are filtered by an online computer cluster. ANTARES instruments a water volume of about 0.015 km³ and is thus intrinsically significantly less sensitive than IceCube. Angular resolutions for ν_μ charged-current and for cascade events with neutrino energies exceeding 10 TeV are better than 0.4° and 2–3°, respectively. Main instrumental systematics are due to the inhomogeneity of detector and deep-sea environment in time, and due to background light from bioluminescence. In spite of its limited size, ANTARES has provided a number of important results, in particular also in common analyses with IceCube, which evidence the importance of full sky coverage for each neutrino flavour and energy. See [27] for a selection of important ANTARES results.

ANTARES has proven the feasibility of deep-sea neutrino detection and has paved the way towards the next-generation neutrino telescope in the Mediterranean Sea, KM3NeT [28]. The KM3NeT 2.0 detector will consist of two installations, ARCA¹ off the eastern Sicilian shore and ORCA² close to the ANTARES site. ARCA will encompass two building blocks with 115 strings each, where each string carries 18 optical modules; the overall instrumented volume will be 1 km³. The prime objective of ARCA is neutrino astronomy in an energy range beyond a few TeV. Due to its larger size and improved detector technology (see below), the angular resolutions in KM3NeT



Figure 8: Photograph of a KM3NeT digital optical module during assembly/testing. Picture provided by the KM3NeT Collaboration.

will be better than in ANTARES ($< 0.1^\circ$ for ν_μ and $< 2^\circ$ for cascade events at energies of about 100 TeV and above). ORCA will use the same basic detector technology as ARCA, but be much more densely instrumented (115 strings, 18 optical modules per string, instrumented volume 0.06 km³). ORCA [29] will focus on neutrino oscillation physics with atmospheric neutrinos in the energy range of a few GeV to a few 10 GeV, and in particular on measuring the neutrino mass ordering. An option to investigate CP violation by directing a neutrino beam from Protvino to ORCA (P2O) [30] is under discussion.

A number of new technical developments has been achieved for KM3NeT that improve functionality, cost-effectiveness, risk mitigation and construction time. Amongst them are equipressure vertical cables (electrical leads and optical fibres in an oil-filled hose), a new deployment strategy (strings wound on a spherical structure which is deployed to the sea floor and then unfurls upon release), and a multi-PMT digital optical module (see Fig. 8). The advantages of the latter are increased photocathode area per glass sphere at reduced overall PMT cost; reduced risk due to less feed-through holes in the glass spheres; better photon-counting; angular information; almost isotropic sensitivity. The construction of both KM3NeT detectors has begun and is expected to be completed 2021/22. A further extension with four more ARCA blocks is envisioned but not yet negotiated. See [27] for expected KM3NeT sensitivities, in particular to a diffuse cosmic neutrino flux as observed by IceCube and to the neutrino mass ordering.

A third large neutrino telescope, the Gigaton Volume Detector (GVD), is currently under construction in Lake Baikal, Russia. It will consist of 8-string clusters with a diameter of 120 m and a height of 525 m; the depth at the installation site is 1360 m. Each string carries 36 optical modules equipped with 10-inch, downward-looking PMTs. In a first phase, 8 clusters will be deployed to instrument 0.4 km³ of water; the final goal are 27 clusters covering a volume of 1.5 km³. Currently three clusters are operational, and two more are to be deployed per year. First results from GVD have been reported at the Neutrino Conference 2018 [31].

¹Astroparticle research with cosmics in the abyss

²Oscillation research with cosmics in the abyss

3.3. Other neutrino detectors

A new approach to detecting highest-energy ν_τ is the use of IACTs (see Sect. 2) directed on the sea surface or other surface areas of the Earth. The basic principle is that ν_τ enter the Earth under zenith angles close to 90° , undergo a charged-current reaction and produce a τ^\pm that enters the atmosphere and initiates an extended air shower upon its decay. A first study of this option has been performed with MAGIC [32, 33]; other experimental approaches to detect tau neutrinos through the same mechanism are discussed in [34].

4. Cosmic-ray and hybrid detectors

In several large detector infrastructures, Cherenkov detection is combined with other measurement methods, such as the observation of fluorescence light, direct particle detection with scintillator or other instruments, or radio detection. Corresponding hybrid infrastructures are typically targeting cosmic rays, in several cases in combination with gamma-ray and/or neutrino measurements.



Figure 9: Photograph of a water Cherenkov detector (foreground) and a building housing six fluorescence telescopes (background) of the Auger infrastructure. Picture provided by the Auger Collaboration.

The largest hybrid detector system to date is the Pierre Auger Observatory (“Auger”) [35] in Argentina, combining 1660 PMT-equipped water tanks on a 3000 km^2 area for the direct detection of charged particle from air showers with 27 fluorescence telescopes observing the atmosphere above the ground array (see Fig. 9). Auger targets cosmic rays with energies of about $10^{17.5}$ – 10^{21} eV and searches for gamma-rays and neutrinos in the same energy interval. The water detectors yield a measurement of the “footprint” of an air shower, from which the energy can be inferred, and act as timing arrays (see Sect. 2.4) for the direction measurement. They have a duty cycle of close to 100%. The fluorescence telescopes measure the light intensity along the shower and, in stereoscopic observations, determine shower position and direction. They thus provide an independent determination of energy and direction, which is cross-calibrated against and combined with the

array measurement. Even though the fluorescence telescopes can only be operated in clear, moon-less nights and thus have a limited duty cycle, their contribution to the control of systematics and thus to the resulting experimental precision is essential.

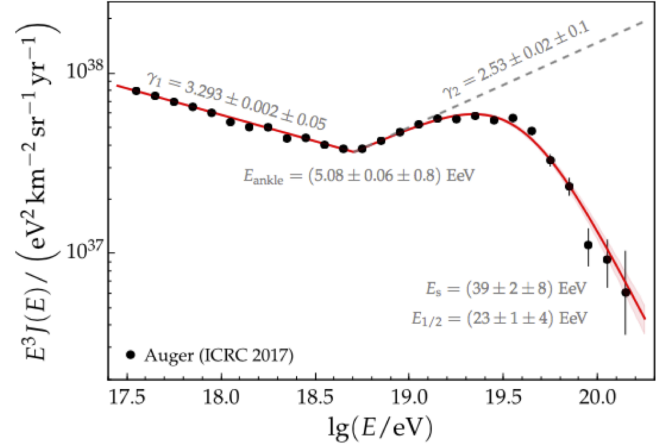


Figure 10: Cosmic-ray energy spectrum beyond $10^{17.5}$ eV measured by Auger. The power-law behaviour below and above the “ankle” is indicated by the dashed lines. Beyond $10^{19.2}$ eV the spectrum steeply decreases. Picture from [36].

Auger started operation with a partial installation in 2001 and has achieved major breakthroughs, amongst others a precise measurement of the cosmic ray spectrum above $10^{17.5}$ eV indicating a clear cut-off beyond $10^{19.2}$ eV (see Fig. 10), and the first detection of a dipole anisotropy of the arrival direction of cosmic rays at highest energies ($E > 8 \times 10^{18}$ eV) [37]. See [38] for a summary of these and further recent results. Still, important questions remain open, amongst them the chemical composition of cosmic rays, the origin of said anisotropy, and the detection of cosmogenic gamma-rays from interactions of highest-energy protons/nuclei with the cosmic microwave background. Auger is currently upgraded to “AugerPrime” with new fast electronics and in particular with scintillator detectors on top of the Cherenkov tanks to improve the discrimination between hadronic and leptonic shower components on ground.

The Tunka experiment in the Tunka valley near Lake Baikal and its current extension stage TAIGA (Tunka Advanced Instrument for cosmic ray physics and Gamma Astronomy) [39, 40] comprise five different detector systems: An array of 133 PMTs observing the sky at clear moon-less nights (Tunka-133), a radio array (Tunka-Rex), an array of 18 scintillation stations recording charged particles (Tunka-Grande, see also [41]), 55 wide-angle Cherenkov stations providing improved Cherenkov light detection (TAIGA-HiSCORE) and several IACTs under construction (TAIGA-IACT).

A different type of hybrid detector is NEVOD [42], a comparatively small ground-level installation in Moscow, Russia. It is unique in combining a 2.1 kton water volume observed by photomultipliers in 91 multi-PMT optical modules with additional scintillator detector tiles for calibration and streamer tube tracking planes for precisely measuring the trajectories

of muons or muon bundles. The combination of muon tracking and Cherenkov measurements offers promising options to cross-check simulations and calibrate e.g. acceptances of optical modules. Also, the simultaneous measurement of muon directions and energies (via the Cherenkov intensity) can be interesting for cosmic-ray studies. See [43] for more details.

Future hybrid approaches are the LHAASO project in China, targeting gamma-rays [44], and the space missions JEM-EUSO [45] and POEMMA [46], both targeting ultra-high energy cosmic rays and neutrinos.

5. Conclusion and Outlook

Cherenkov detectors play a crucial role in gamma-ray, neutrino and cosmic-ray astroparticle physics. Many of the recent breakthrough-results would not have been possible without them, and they are essential for the future experiments being constructed or planned.

References

- [1] P.A. Cherenkov, Visible luminescence of pure liquids under the influence of γ -radiation, Dokl. Akad. Nauk SSSR 2 (1934) 451. [doi:10.3367/UFNr.0093.196710n.0385](#).
- [2] I.M. Frank and I.E. Tamm, Coherent visible radiation of fast electrons passing through matter, Compt. Rend. Akad. Sci. URSS 14 (1937) 109. [doi:10.3367/UFNr.0093.196710o.0388](#).
- [3] F.C.T. Barbato et al., Another step in photodetection innovation: the 1-inch vsipmt prototype, in: this issue.
- [4] S. Vinogradov, Status and perspectives of solid state photon detectors, in: this issue.
- [5] M. Ziembicki, Photosensors and front-end electronics for the hyper-kamiokande experiment, in: this issue.
- [6] A. Sidorenkov et al., Development of medium and small size photomultipliers for cherenkov and scintillation detectors in astroparticle physics experiments, in: this issue.
- [7] S. Funk, Ground- and space-based gamma-ray astronomy, Ann. Rev. Nucl. Part. Sci. 65 (2016) 245. [doi:10.1146/annurev-nucl-102014-022036](#).
- [8] H.E.S.S. Collaboration. [H.E.S.S. web page](#) [online, cited 12 Nov 2018].
- [9] MAGIC Collaboration. [MAGIC web page](#) [online, cited 12 Nov 2018].
- [10] Veritas Collaboration. [Veritas web page](#) [online, cited 12 Nov 2018].
- [11] T.C. Weekes et al., Observation of TeV gamma rays from the Crab nebula using the atmospheric Cherenkov imaging technique, Astrophys. J. 342 (1989) 379. [doi:10.1086/167599](#).
- [12] S.M. Bradbury et al., HEGRA Collaboration, Detection of γ -rays above 1.5 TeV from Mkn 501, Astron. Astrophys. 320 (1997) L5.
- [13] FACT Collaboration. [FACT web page](#) [online, cited 12 Nov 2018].
- [14] J.A. Barrio, for the CTA Consortium, Status of the large size telescopes and medium size telescopes for the Cherenkov Telescope Array observatory, in: this issue.
- [15] M. Heller, for the CTA Consortium, Status and perspectives of the small size telescopes for the Cherenkov Telescope Array southern observatory, in: this issue.
- [16] HAWC Collaboration. [HAWC web page](#) [online, cited 13 Nov 2018].
- [17] A.U. Abeysekara et al., HAWC Collaboration, Extended gamma-ray sources around pulsars constrain the origin of the positron flux at Earth, Science 358 (2017) 911. [doi:10.1126/science.aan4880](#).
- [18] U.F. Katz and C. Spiering, High-energy neutrino astrophysics: Status and perspectives, Prog. Part. Nucl. Phys. 67 (2012) 651. [doi:10.1016/j.pnpnp.2011.12.001](#).
- [19] Super-Kamiokande Collaboration. [Super-Kamiokande web page](#) [online, cited 13 Nov 2018].
- [20] SNO Collaboration. [SNO web page](#) [online, cited 13 Nov 2018].
- [21] Y. Takeuchi, for the Super-Kamiokande Coll., Recent results and future prospects of Super-Kamiokande, in: this issue.
- [22] K.A. Olive et al., Particle Data Group, The review of particle physics, Chin. Phys. C 38 (2014) 090001.
- [23] B. Aharmim, SNO Collaboration, Electron energy spectra, fluxes, and day-night asymmetries of B-8 solar neutrinos from measurements with NaCl dissolved in the heavy-water detector at the Sudbury Neutrino Observatory, Phys. Rev. C 72 (2005) 055502. [doi:10.1103/PhysRevC.72.055502](#).
- [24] IceCube Collaboration. [IceCube web page](#) [online, cited 13 Nov 2018].
- [25] D. Williams, for the IceCube Coll., Status and prospects for the IceCube neutrino observatory, in: this issue.
- [26] D. Williams, for the IceCube Collaboration, Recent results from IceCube, Int. J. Mod. Phys. (Conf. Ser.) 46 (2018) 1860048. [doi:10.1142/S2010194518600480](#).
- [27] T. Chiarusi, for the ANTARES and KM3NeT Coll., Neutrino astronomy and oscillation research in the mediterranean: ANTARES and KM3NeT, in: this issue.
- [28] S. Adrin/Martinez et al., KM3NeT Collaboration, Letter of intent for KM3NeT 2.0, J. Phys. G 43 (2016) 084001. [doi:10.1088/0954-3899/43/8/084001](#).
- [29] J. Brunner, for the KM3NeT Collaboration, KM3NeT-ORCA, PoS NEUTEL2017 057. [doi:10.22323/1.307.0057](#).
- [30] D. Zaborov for the KM3NeT Collaboration, [The KM3NeT neutrino telescope and the potential of a neutrino beam from Russia to the Mediterranean Sea](#), Contribution to 18th Lomonosov Conference on Elementary Particle Physics, Moscow, 2017 (2018). URL [arxiv.org/abs/arXiv:1803.08017](#)
- [31] Z. Dzhilkibaev for the Baikal-GVD Collaboration, [Baikal-GVD – the next-generation neutrino telescope in Lake Baikal](#), Contribution to 28th Int. Conf. on Neutrino Physics and Astrophysics, 2018, Heidelberg, Germany (2018). [doi:10.5281/zenodo.1302982](#). URL [zenodo.org/record/1302982](#)
- [32] R. Mirzoyan et al., Extending the observation limits of imaging air Cherenkov telescopes toward horizon, in: this issue.
- [33] M.L. Ahnen et al., MAGIC Collaboration, Limits on the fluxes of tau neutrinos from 1 PeV to 3 EeV with the MAGIC telescope, Astropart. Phys. 102 (2018) 77. [doi:10.1016/j.astropartphys.2018.05.002](#).
- [34] J. Alvarez-Muñiz et al., A comprehensive approach to tau-lepton production by high-energy tau neutrinos propagating through Earth, Phys. Rev. D 97 (2018) 023021. [doi:10.1103/PhysRevD.97.023021](#).
- [35] Pierre Auger Collaboration. [Pierre Auger web page](#) [online, cited 18 Nov 2018].
- [36] Pierre Auger Collaboration, [The Pierre Auger Observatory: Contributions to the 35th International Cosmic Ray Conference \(ICRC 2017\)](#), collection of conference contributions (2017). URL [arxiv.org/abs/arXiv:1708.06592](#)
- [37] A. Aab et al., Pierre Auger Collaboration, Large-scale cosmic-ray anisotropies above 4 EeV measured by the Pierre Auger Observatory 868 (2018) 4. [doi:10.3847/1538-4357/aac689](#).
- [38] I. Maris, for the Pierre Auger Coll., Cherenkov detection at the Pierre Auger Observatory, in: this issue.
- [39] TAIGA Collaboration. [TAIGA web page](#) [online, cited 18 Nov 2018].
- [40] N. Budnev et al., TAIGA – a hybrid array for high-energy gamma astronomy and cosmic ray physics, EPJ Web Conf. 191 (2018) 01007. [doi:10.1051/epjconf/201819101007](#).
- [41] A. Vaidyanathan et al., Optimization of electromagnetic and hadronic extensive air showers identification using muon detectors of TAIGA experiment, in: this issue.
- [42] NEVOD Collaboration. [NEVOD web page](#) [online, cited 18 Nov 2018].
- [43] A. Petrukhin, Cherenkov water detector NEVOD and its further development, in: this issue.
- [44] S. Vernetto, for the LHAASO Collaboration, Gamma-ray astronomy with LHAASO, J. Phys. Conf. Ser. 718 (2016) 052043. [doi:10.1088/1742-6596/718/5/052043](#).
- [45] JEM-EUSO-Collaboration. [JEM-EUSO web page](#) [online, cited 18 Nov 2018].
- [46] A. Olinto et al., POEMMA: Probe of extreme multi-messenger astrophysics, PoS ICRC2017 542. [doi:10.22323/1.301.0542](#).